Monteagudo, Silvia M.; Casati, María Jesus; Gálvez, Jaime C.

Influence of the bed joint thickness on the bearing capacity of the brick masonry under compression loading: an ultrasound assessment

Revista de la Construcción, vol. 14, núm. 1, 2015, pp. 9-15

Pontificia Universidad Católica de Chile

Santiago, Chile

Influence of the bed joint thickness on the bearing capacity of the brick masonry under compression loading: an ultrasound assessment

Influencia del espesor de la junta de mortero en la capacidad de resistencia de la mampostería de ladrillo bajo cargas de compresión: una evaluación de ultrasonido.

Silvia M. Monteagudo (Main Autor)
Universidad Politécnica de Madrid
Escuela Técnica Superior de Caminos, Canales y Puertos,
Departamento de Ingeniería Civil
sm.monteagudo@gmail.com

Jaime C. Gálvez
Universidad Politécnica de Madrid
Escuela Técnica Superior de Caminos, Canales y Puertos,
Departamento de Ingeniería Civil
jaime.galvez@upm.es

María Jesus Casati (Contact Autor)
Universidad Politécnica de Madrid
Escuela Universitaria de Ingeniería Técnica Aeronautica,
Departmento de Vehículos Aeroespaciales.
mariajesus.casati@upm.es
Fax/Phone: +34 913367503
Pza. Cardenal Cisneros 3, 28040, Madrid (Spain)

Manuscript Code: 210
Date of Reception/Acceptance: 14/03/2014-01/03/2015

Abstract
The aim of this paper is to analyse the influence of mortar bed joint thickness on the structural behaviour of brick-masonry specimens under compressive stress. Moreover, the progressive cracking of the material was studied during the loading process. Nine walls and nine columns were tested, combining three mortar bed joint thicknesses. Simultaneously, ultrasound, extensometer and Schmidt hammer measurements were recorded. The obtained results show that the thinner the mortar bed joint (5mm), the greater the breaking load (20.5N/mm2) and ultrasonic pulse speed. In addition, ultrasound evaluation shows good agreement with the extensometer measurements and allows accurate detection of the inner material failure.

Resumen
En este trabajo se analiza la influencia del espesor de la junta de mortero en la resistencia a compresión de la fábrica de ladrillo cerámico bajo esfuerzos de compresión uniaxial. Además se estudia el progresivo agrietamiento del material durante el proceso de carga. Se han ensayado nueve muros y nueve pilares, combinando tres espesores de junta de mortero realizando medidas con ultrasonidos, además se han realizado medidas con extensómetros y esclerómetro. Los resultados obtenidos muestran que a menor espesor de junta (5mm) se obtiene una mayor carga de rotura (20.5 N/mm2) y mayor valor de la velocidad de pulso ultrasónico. La medida con ultrasonidos muestra una buena correlación con las medidas extensométricas y permite una eficaz detección del agrietamiento interior del material durante el proceso de rotura.

Keywords: Non-destructive tests; ultrasound; brick masonry; compression stress; bed joint.

Palabras Claves: Ensayos no destructivos, ultrasonido, mampostería de ladrillo, esfuerzo a la compresión, juntas de mortero.

Abbreviations: Linear variable differential transformer (LVDT); non-destructive tests (NDT); ultrasonic pulse velocity (UPV).

Introduction

Ceramic brick masonry has been used since ancient times in building and civil engineering construction, with a particularly long tradition in South America. The study of its structural behaviour and strength continues to focus the attention of researchers (Mohammed, 2011; Oliveira et al., 2006; Reyes, 2008; Reyes, 2009). This interest also meets the need to assess the load bearing capacity of historic structures such as bridges and buildings. The restoration of historic buildings, as well as the change of use of other well-preserved structures, requires assessment of their resistance in order to establish the needs of reinforcement or rehabilitation, based on usage requests (Lourenço, 2002; Chavez, 2005). Most of the ancient buildings are masonry constructions.

Furthermore, brick masonry is a heterogeneous and anisotropic material formed by bricks and mortar. Its behaviour up to failure is nonlinear and primarily depends both on its components (brick, mortar and brick-mortar interface) and its constructive disposition (bond and mortar bed joint thickness) (Senthivel, 2009). The normalised calculations available for determining masonry strength lead to significantly different values and neglect important aspects such as bed joint thickness (Monteagudo, 2010).

Intervention in the immovable cultural heritage is required to be as less aggressive as possible (Lombillo, 2007), with use of the non-destructive test (NDT) being an appropriate way to identify the properties of masonry structures. Among the possible NDTs used for mechanical characterisation, the ultrasonic pulse velocity (UPV) measurement is that successfully used in brick (Koroth, 1998) and stone masonries (Vasconcelos, 2008). Moreover, the technique has been also used in combination with other NDTs, such as thermography (Meola, 2005). However, when studying how the thicknesses of mortar bed joints affect the behaviour of brick masonry, the literature offers few results from experimental tests.

This paper analyses the influence of mortar bed joint thickness on the structural behaviour of brick masonry specimens under uniaxial compressive stress. In doing so, nine walls and columns have been tested that entail a combination of three mortar bed joint thicknesses, subjected to compressive load until failure. With the purpose of assessing the progressive cracking of the material during the loading process, NDT tests have been performed, such as UPV measurements. In addition, extensometer and Schmidt hammer measurements have been considered to verify the reliability of the UPV technique.

The first part of the present work was presented at the Spanish Fracture Conference held in 2011 (Monteagudo, 2011). The present paper includes new research advances and a more detailed and deeper discussion, based on the new experimental data. The evolution of the masonry specimens cracking by means of ultrasonic velocity assessment is also included.

Methodology

Design of the tests

Regarding the brick masonry columns and walls, three specimens were manufactured for each mortar bed joint thickness (5, 10 and 15mm). The dimension of the columns was 235x235x800mm, while the dimension of the walls was 750x115mm on plan view. The height of the walls varied between 650 and 830mm. The nomenclature used to designate the specimens is shown in Table 1.

Table 1. Nomenclature of the specimens. Source: self-elaboration.

Joint thickness (mm)	Nomenclature		
Columns			
5	C 1.05	C 2.05	C 3.05
10	C 1.10	C 2.10	C 3.10
15	C 1.15	C 2.15	C 3.15
Walls			
5	W 1.05	W 2.05	W 3.05
10	W 1.10	W 2.10	W 3.10
15	W 1.15	W 2.15	W 3.15

The specimens were subjected to the uniaxial compression test and, simultaneously, measurements of UPV, Schmidt hammer and extensometers were recorded.

Bricks

For the manufacture of the specimens, commercial clay bricks were used. The dimension of the bricks was 235x108x37mm. According to European Standard UNE-EN 772-1, the compressive strength of three brick specimens of 40x40x40mm was σc=59.8N/mm2 (see Table 2).

Mortar

The mortar was made from Portland cement CEM I 42.5N type and standard silica sand with a maximum aggregate size of 1.5mm. The water-to-cement ratio was 0.5 and cement sand ratio was 1/6 (NBE FL-90, 1990). According to the European Standard UNE-EN 1015-11, (UNE-EN 1015-11, 2007), the compressive strength of three mortar specimens with dimensions 35x35x35mm was 22.9N/mm2. Table 2 shows the compressive and flexion strength results of the brick and mortar specimens, as well as the average values.

Table 2. Compressive and flexion strength results on brick and mortar specimens. Source: self-elaboration.

	Specimen	Dimensions (mm)	Fc (kN)	σc (N/mm2)
brick	1	38x38x38	81.2	59.79
	2	40x40x40	103.2	
	3	39x39x39	89.2	
mortar	1	35x35x35	36.0	22.86
	2	35x35x35	23.0	
	3	35x35x35	25.0	

Manufacture of the columns and the walls

In order to ensure a uniform moisture degree and avoid the possible absorption of water from the mortar by the brick, which could cause poor adhesion in the brick-mortar interface, before the manufacture of the specimens the bricks were dipped into water for one hour. The walls and columns were prepared with three joint thicknesses of 5, 10 and 15 mm. The top and bottom surfaces of the specimens were finished with a 20mm-thick layer of mortar. For providing plane surface on the end, the support base was capped with sulphur mortar.

Specimen test procedure

The nine walls and columns were tested under compression according to the European Standard UNE-EN 1052-1. The test was performed with a servo-hydraulic testing machine with 2000kN capacity and displacement control. In order to guarantee uniform load distribution, 1cm-thick chipboard was inserted between the plate of the load actuator and the specimen. In the case of the walls, a HEB250 steel beam was used. The contact of this beam with the wall was also made through 1cm-thick chipboard which was adjusted to the area of the wall base. The load was applied in load stages of 150kN, with deformation stabilisation at each stage.

Shortening of the specimen during the test was measured by LVDT extensometers with 40mm span. In the columns, two extensometers were attached on opposite sides by a steel frame fastened with screws Figure 1. Furthermore, four extensometers were attached to the walls, two on each face, by means of a methacrylate flange (Figure 2).

Figure 1. Compressive strength test in columns. Source: self-elaboration.

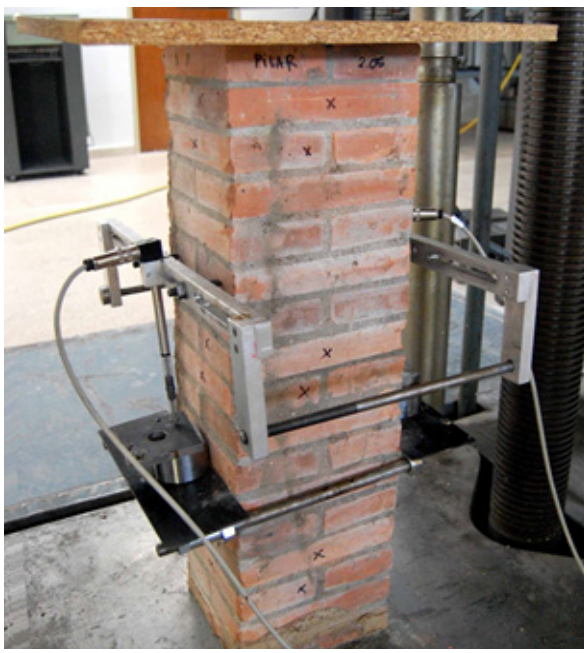

During the loading process, and for each load stage of 150kN, UPV measurements were taken simultaneously by means of Pundit ultrasound equipment with high frequency transducers (50-100kHz). In the case of the columns, UPV was measured in two directions (see Figure 3). In position one the wave passes through brick and mortar (B+M) and in position two through single brick (B). These measurements were taken in both X and Y-axis directions. As regards the walls, the measurement was carried out through single brick, without passing through

mortar, as shown in Figure 4. Measurements were taken at three different heights in both the columns and the walls.

In addition, a Schmidt hammer was used to obtain an order of magnitude of the surface hardness variation on brick and mortar, during the loading of the columns. For this purpose, six measurements at different heights were taken.

Figure 2. Compressive strength test in walls. Source: self-elaboration.

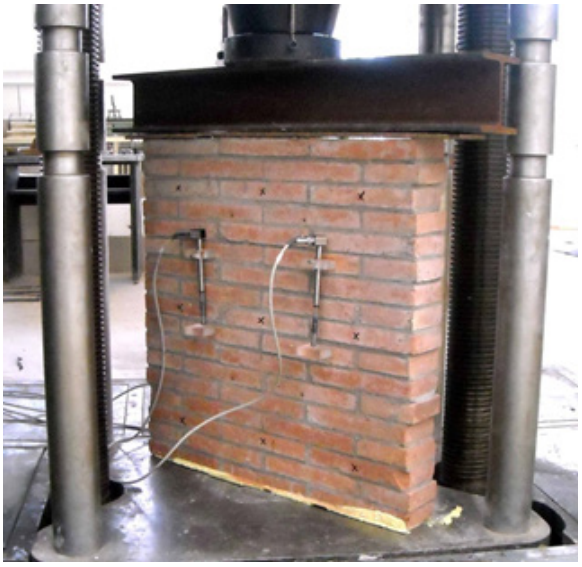

compaction of the material that reduces the volume of voids. After exceeding the maximum breaking load, the appearance of cracks is shown by a sharp decrease in the UPV (Figures 5.a and 5.b). During continuous monitoring of structures, the decrease of ultrasonic pulse can be a clear indication of the appearance of internal cracks that may not have been manifested on the outside. Meglis et al. (Meglis, 2005) also observed a decrease in the average UPV as cracks propagated.

Figure 4. Scheme of the UPV transducers in the walls. Source: self-elaboration.

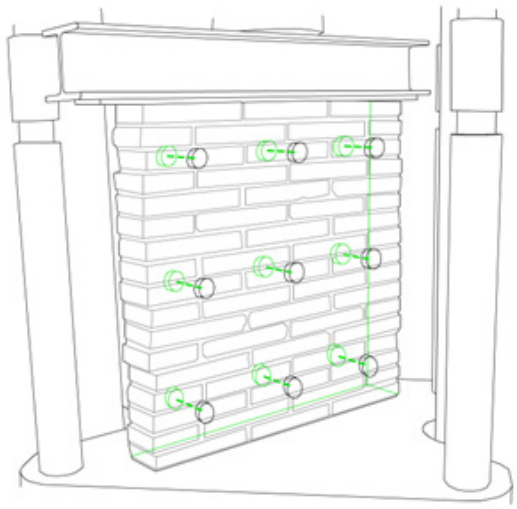

Figure 3. Scheme of the transducer position in the column UPV measurement. Source: self-elaboration.

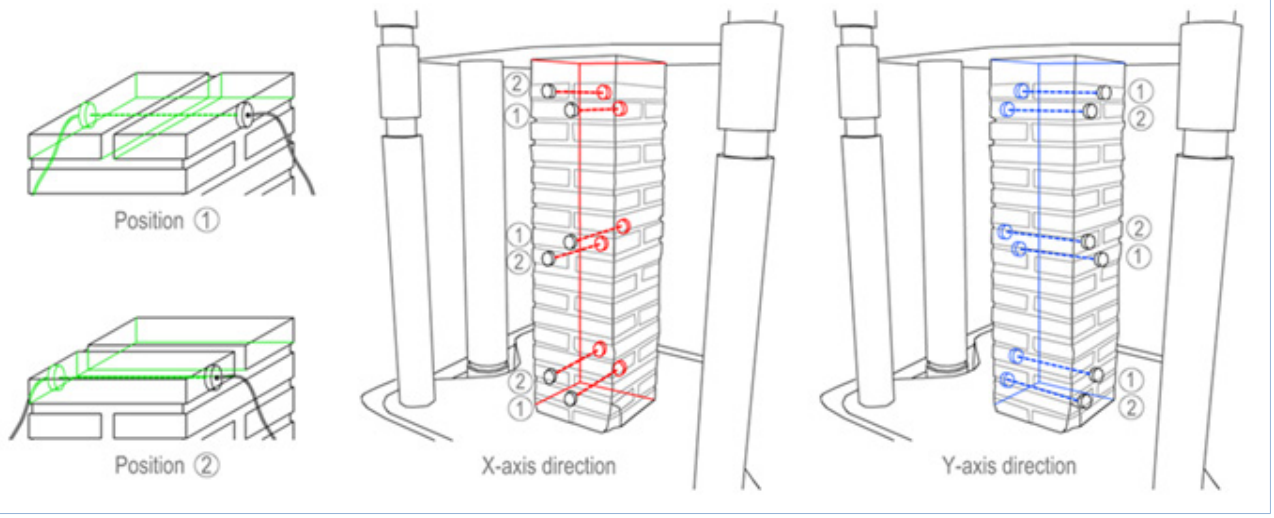

Results and discussion

Figure 5.a shows the average UPV measurements taken in the columns depending on the applied load for the two aforementioned positions (see Figure 3) and three joint thicknesses. Figure 5.b shows similar results for the walls. Regarding the UPV in the columns, as shown in Figure 5.a, the average value is clearly lower when the wave passes through brick and mortar. The average UPV for the position 1 (B+M) was 3,863.2 m/s, while the average UPV for the position 2 (B) was 4,236.5 m/s. This is primarily due to the lower stiffness of the joint and presence of a discontinuity between the brick and the mortar. Before the maximum breaking load a slight increase in the UPV, for both the columns and walls, was observed. This phenomenon has been noted by various authors (Koroth, 1998), (Schuller, 1997). The increase is due to the greater

Figure 6.a compares the average UPV of the columns for the various mortar bed joint thickness (5, 10 and 15mm) at each load stage. In addition, Figure 6.b shows similar results for the walls. For both the columns and walls, a clear relationship is seen between the UPV and the thickness of the mortar bed joint. The UPV measurement is higher in all the specimens with a lower mortar bed joint. Such an effect is due to the higher deformability of the mortar compared with that of the brick. Mortar deformation introduces tensile stresses that are transmitted to the brick through the mortar-brick interface. Moreover, the stiffness of the brick leads to a lower fracture load of the masonry.

Figure 5. UPV depending on the load, a) in columns and b) in walls. Source: self-elaboration.

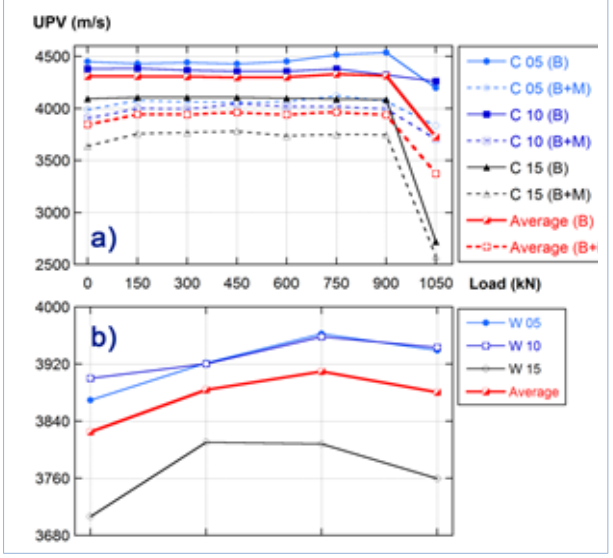

The experimentally measured average strength of the specimens is shown in Table 3, in which the maximum rupture stresses for the columns and walls are listed. The individual values for each mortar bed joint thickness correspond to the average value of the three specimens tested. An increase in resistance, especially in the walls, is notable as the mortar bed joint thickness decreases. Lastly, the characteristic strength of the brick masonry has been obtained from the strength of its constituents. In order to obtain the resistance of the columns and the walls, among the experimental formulae available in the literature, that offered by Haller (1969) is widely accepted (see Eq. 1).

$$R_M = (\sqrt{1 + 0.15R_L} - 1)(8 + 0.057R_m) \quad (1)$$

Where, R_L and R_m are the brick and mortar strength respectively and R_M is the masonry strength, all in kg/cm^2.

Through applying Eq. 1 to the experimentally values of Table 2 a wall strength of 17.9N/mm2 was obtained. From the data presented in Table 3, it may be concluded that the formula offered by Haller is well suited in calculating the compressive strength of the columns, though it is not so suitable in calculating the compressive strength of the walls as it fails to consider wall slenderness. This equation could only be used in cases where the wall has a large thickness and in which, therefore, slenderness is lower.

In Table 4 f_k is the masonry characteristic strength, f_b and f_m are the normalized compressive strengths of the brick and the mortar respectively, all in N/mm2, K is a constant value which varies between 0.5 to 0.6 in mm2/N depending on the presence of stitches, f is the average strength, f_j is the strength of each individual test, δ is the standard deviation and n is the number of specimens tested.

The analytical values obtained by EC-6 and CTE allow the calculation of the characteristic compressive strength based on the compression strength of the constituent materials. Furthermore, this provides similar values to the experimental average obtained in the columns. Although the NBE FL-90 is repealed, it is included in the comparison since many brick buildings that are currently in service, have been calculated according to its requirements The advantage provided by this standard is the use of experimental values to calculate the characteristic strength of the masonry. Should these preliminary tests not be made, the norms propose establishing of the characteristic strength of the wall depending on the type and individual strength of the constituent materials and mortar bed joint thickness. Once again, the accuracy of this standard is greater despite only walls being considered.

Figure 6. UPV average measurements for each mortar bed joint thickness depending on the load, a) in columns and b) in walls. Source: self-elaboration.

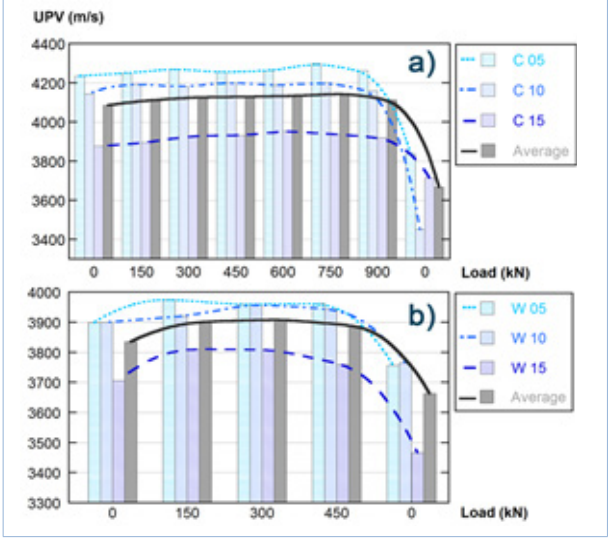

Table 3. Average breaking strength of the specimens tested. Source: self-elaboration.

Mortar bed joint (mm)	Breaking strength (N/mm2)	Individual	Average
Columns	05	20.5	19.5
	10	19.1	
	15	19.0	
Walls	05	10.4	7.8
	10	7.7	
	15	5.3	

Table 4. Average characteristic compressive strength obtained by analytical expressions. Source: self-elaboration.

Standard	Characteristic compressive strength (N/mm2)	
EC-6 CTE	$f_k = K f_b^{0.65} f_m^{0.25}$ $K = 0.60$ $f_m < 20MPa$ $f_m < 2f_b$	$f_{k\,WALLS} = 18.74$
CTE	$f_k = f - 1{,}64\delta$ $\delta = \sqrt{\frac{\sum(f_j - f)^2}{n-1}}$	$f_{k\,COLUMNS} = 18.12$ $f_{k\,WALLS} = 3.62$

When design calculations proposed by the aforementioned standards are compared with the experimental results, the calculations of the projected masonries are, in all cases, somewhat conservative, especially when the mortar bed joint thickness is below 10mm. Despite the precautions taken, the lower bearing capacity of the walls, relative to that of the columns, is due to the slenderness and may induce an eccentricity of the load. By means of real scale specimens, Carpinteri et al. have verified that the breaking strength is inversely proportional to slenderness (Carpinteri, 2007).

Figure 7. UPV depending on the height, a) in C05 column and b) in W05 wall. Source: self-elaboration.

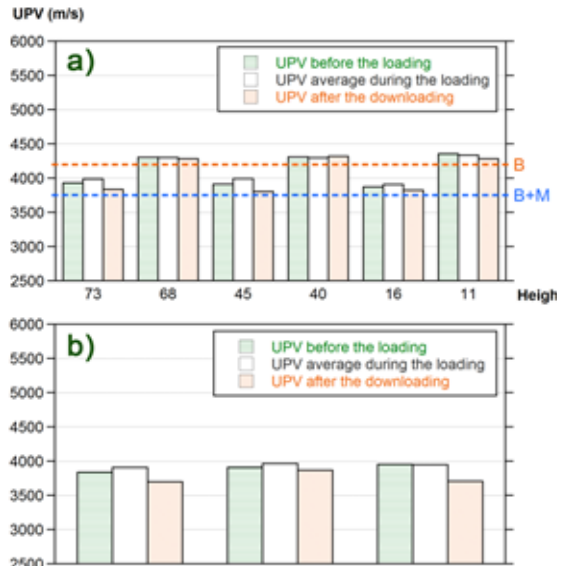

Figure 7.a shows the average UPV in the columns with a 5mm mortar bed joint for the two positions described in Figure 3: position 1 (B+M) and 2 (B), while Figure 7.b presents similar results for the walls with a mortar bed joint of 5mm. The obtained values for the columns and walls with mortar bed joint thicknesses of 10 and 15 mm showed similar results. In both figures the UPV is represented depending on the height and the moment in which the measure was taken (before, during or after the loading test). It is observed that the measurement of values depending on different heights shows slight variation, which confirms a uniform load distribution on the test specimens.

Figure 8 represents the average Schmidt hammer rebound index in the brick and mortar columns, depending on the various load stages. The rebound index is higher in the brick than in the mortar; this was expected due to the higher stiffness of the brick, as shown by the surface hardness. One notable variable is a tendency to increase the Schmidt hammer rebound index as the load increases that could be explained by the acquisition of compactness of the material. This increase is more pronounced in the mortar than in the brick, with the mortar being more deformable. Evaluation of the surface hardness confirms the findings obtained by the UPV measures as shown in Figure 8.

Figure 8. Average Schmidt hammer rebound index in columns. Source: self-elaboration.

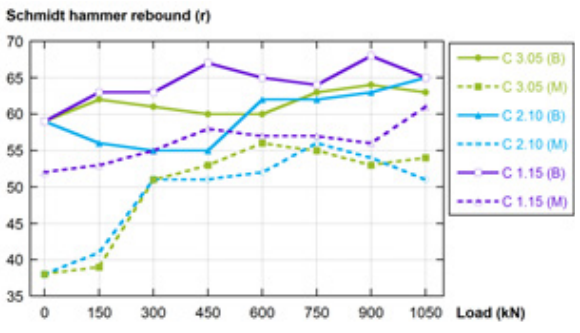

Moreover, the value of the UPV can be also indicative of the occurrence of internal cracks in the structure. As shown in Figure 9, there is a decrease in the Y-axis UPV measure for the specimen C1.05 from a load of 900N. This reduction corresponds to the appearance of a crack in the transverse direction (X-axis direction). Conversely, in the specimen C 1.10 the crack appeared in the opposite direction (Y-axis) and, therefore, the UPV wave decreases in the X-axis direction. Finally, the specimen C 3.15 has not produced any significant crack that interferes with the measures and, thus, the variation of the ultrasonic pulse is similar in each direction.

Figures 10.a and 10.b show stress-strain curves measured by means of extensometers in the columns and walls respectively. The stress-strain curves of the columns (Figure 10.a) show low experimental scattering and confirm a greater deformability of the columns with a thicker mortar bed joint. In the case of the walls (Figure 10.b) the results are similar, although there is a greater scattering attributable to wall slenderness and buckling problems (Sandoval, 2012).

Figure 10. Stress-strain curves, a) in columns and b) in walls. Source: self-elaboration.

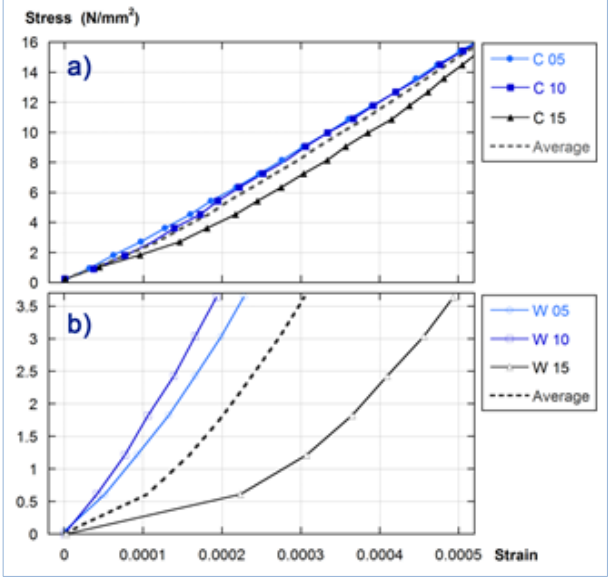

Conclusions

Apart from the previously mentioned results, the conclusions to be drawn from this research are as follows:

From a methodological point of view non-destructive evaluation methods used during the experimental campaign offer reliable information on the deterioration and bearing status of the brick masonry. The continuing UPV measurement, complemented by the Schmidt hammer, are useful methods for assessing the structure without damaging the existing material. With proper calibration, the ultrasonic method can be useful, especially when the damaged areas are not detectable on visual inspection.

Regarding the compression strength results, there is a direct relationship between the thickness of the mortar bed joint and the bearing capacity of the masonry. As explained above, the smaller the thickness of the mortar bed joint the greater is the UPV registered.

The compressive strength of constituent materials determines the masonry strength; however, they alone do not allow

definitive conclusions about masonry compressive strength to be established. The models of the current standards establish the nominal strength depending on the constituent materials; nevertheless, aspects such as the thickness of the mortar bed joints are crucial in the nonlinear behaviour of brick masonry structures.

Acknowledgments

The authors wish to express their gratitude to the Ministerio de Economía and Competitividad for the grant DPI 2011-24876..

References

Carpinteri, A. & Lacidogna, G. (2007). Damage evaluation of three masonry towers by acoustic emission. Engineering Structures, 29(7), 1569–1579.

Chavez, J.A., & Álvarez, O. (2005). Metodología para el diagnóstico y restauración de edificaciones. Revista de la Construcción, 4(2), 47-54.

CTE (2008). Código Técnico de la Edificación, Partes I y II. Ministerio de Vivienda, Spain.

EC-6 UNE-EN 1996-1-1:2011+A1 (2013). Eurocode 6: Design of masonry structures. Part 1-1: General rules for reinforced and unreinforced masonry structures.

Haller, C. (1969). Load capacity of brick masonry. Designing, Engineering and Constructing with Masonry Products, FB Johnson Ed.

Koroth, S.R., Fazio, C., & Feldman, D. (1998). Evaluation of clay brick durability using ultrasonic pulse velocity. Journal of Architectural Engineering, 4, 142-147.

Lombillo I., Villegas, L., Silió, D., Hoppe, C., & GTED-UC. (2008). Evaluación no destructiva del patrimonio construido. Revista Internacional Construlink, 16(6), 40-53.

Lourenço C.B. (2002). Computations on historic masonry structures. Progress in Structural Engineering and Materials 4(3), 301-319.

Meglis I.L., Chow T., Martin C.D., & Young R.C. (2005). Assessing in situ microcrack damage using ultrasonic velocity tomography. International Journal of Rock Mechanics and Mining Sciences, 42(1), 25–34.

Meola C.l., Di Maio, R., Roberti, N., & Carlomagno, G.M. (2005). Application of infrared thermography and geophysical methods for defect detection in architectural structures. Engineering Failure Analysis, 12, 875–892.

Mohammed A., Hughes T.G., & Mustapha A. (2011). The effect of scale on the structural behavior of masonry under compression. Construction and Building Materials, 25(1), 303-307.

Monteagudo S.M. (2010). Análisis estructural de muros de fábrica mediante ensayos no destructivos, Proyecto Fin de Máster. E.T.S. Ingenieros Caminos, Canales y Puertos, Universidad Politécnica Madrid.

Monteagudo S.M., Casati M.J., Gálvez J.C., Kratochvil J., & Al-Assadi G. (2011). Evaluación estructural mediante ultrasonidos del efecto del espesor de la junta de mortero en muros de fábrica de ladrillo cerámico sometidos a esfuerzos de compresión hasta su rotura. Anales de Mecánica de Fractura, 28(1), 149-154.

NBE FL-90 (1990). Norma Básica de la Edificación: Muros resistentes de fábrica de ladrillo, Ministerio de Obras Públicas y Urbanismo de España, Spain.

Oliveira, D.V., Lourenço, C.B. & Roca, C. (2006). Cyclic behaviour of stone and brick masonry underuniaxial compressive loading. Materials and Structures, 39(2), 219-227.

Reyes E., Casati M.J., & Gálvez J.C. (2008). Cohesive crack model for mixed mode fracture of brick masonry. International Journal of Fracture, 151 (1), 29-55.

Reyes E., Gálvez, J.C., Casati, M.J., Cendón, D.A., Sancho, J.M., & Planas, J. (2009). An embedded cohesive crack model for finite element analysis of brickwork masonry. Engineering Fracture Mechanics, 76(12), 1930-1944.

Rolando, A. (2006). Resistencia característica a compresión de una fábrica de ladrillo en función de la resistencia de sus componentes - Comprobación experimental de expresiones analíticas de la normativa europea. Escuela Técnica Superior de Arquitectura de la Universidad Politécnica de Madrid. Materiales de Construcción, 283(56), 91-98.

Sandoval, C., & Roca, C. (2012). Study of the influence of different parameters on the buckling behaviour of masonry walls. Construction and Building Materials, 35, 888-899.

Schuller M., Berra M., Atkinson R., & Binda, L. (1997). Acoustic tomography for evaluation of unreinforced masonry. Construction and Building Materials, 11(3), 199-204.

Senthivel R., & Lourenço P.B. (2009). Finite element modelling of deformation characteristics of historical stone masonry shear walls. Engineering Structures, 31(9), 1930-1943.

UNE-EN 772-1 (2011). Methods of test for masonry units. Part 1: Determination of compressive strength, Spain.

UNE-EN 1015-11 (2007). Methods of test for mortar for masonry. Part 11: Determination of flexural and compressive strength of hardened mortar, Spain.

UNE-EN 1052-1 (1999). Methods of test for masonry. Part 1: Determination of compressive strength, Spain.

Vasconcelos, G., Lourenço, P.B., Alves, C.A.S., Pamplona, J. (2008). Ultrasonic evaluation of the physical and mechanical properties of granite. Ultrasonics, 48(5), 453–466.

Figure 9. UPV depending on the load and scheme of the specimens rupture. Source: self-elaboration.